2.2um BSI CMOS image sensor with two layer photo-detector

H.Sasaki, A.Mochizuki, Y.Sugiura, R.Hasumi, K.Eda, Y.Egawa, H.Yamashita, K.Honda, T.Ohguro, H.S.Momose, H.Ootani, Y.Toyoshima, and T.Asami
Toshiba Corporation Semiconductor & Storage Products Company,
1 Toshiba-cho, Komukai, Saiwai-ku, Kawasaki, Japan 212-8583
E-mail: hiroki8.sasaki@toshiba.co.jp

ABSTRACT

Back Side Illumination (BSI) CMOS image sensors with two-layer photo detectors (2LPDs) have been fabricated and evaluated. The test pixel array has green pixels (2.2um x 2.2um) and a magenta pixel (2.2um x 4.4um). The green pixel has a single-layer photo detector (1LPD). The magenta pixel has a 2LPD and a vertical charge transfer (VCT) path to contact a back side photo detector. The 2LPD and the VCT were implemented by high-energy ion implantation from the circuit side. Measured spectral response curves from the 2LPDs fitted well with those estimated based on light-absorption theory for Silicon detectors. Our measurement results show that the keys to realize the 2LPD in BSI are; (1) the reduction of crosstalk to the VCT from adjacent pixels and (2) controlling the backside photo detector thickness variance to reduce color signal variations.

Keywords: image sensor, BSI, two-layer photo-detector, color signal variation

1. INTRODUCTION

Multi-layer photo detector pixel in CMOS imagers is one of the alternative color acquisition solutions to conventional 1LPDs solution. In a multi-layer photo detector pixel, multi-layer photo detectors are stacked in Si and multiple color information is acquired per pixel, although single color information is acquired per pixel in a widely used 1LPD with a Bayer CFA [1]. Several reports both on triple-layer photo detector solutions and on 2LPD solutions have already been reported and low color aliasing for high spatial frequency images have been attained [2][3][4][5]. For a recent small size pixel, the low light signal-to-noise ratio (SNR) is an important limiting factor for a pixel size shrink. The low light SNR is dominated by photon shot noise, and increasing the number of photons that the photo-detector can be received is the only way to improve a luminance SNR (YSNR). Multi-layer photo detector architecture is one candidate to improve low light SNR, since more photons can be utilized in a single pixel because photons from wider light spectral band can be absorbed in multi-layer photo detector architecture. Theoretical investigations of a YSNR improvement for small pixels suggested that the magenta-green CFA checker pattern with the 2LPDs is one of the possible solutions to improve the low-light SNR [6]. This paper reports on a study of 2LPDs structure implemented in BSI architecture to see a feasibility of small pixel 2LPDs as a possible solution for better low light SNR

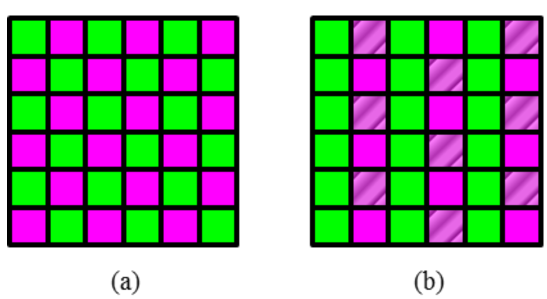

Figure 1.1 CFA patterns, (a) Mg-G Checker Pattern, (b) Our test Pattern; the VCT is covered with light shield metal.

A 2.2um BSI CMOS imager with a 2LPD test pixel array with a magenta-green color filter array (CFA) has been fabricated and evaluated. Magenta pixel has blue/red 2LPDs and VCT path for blue photo-detectors implemented on back-side Si surface. Figure 1.1 shows the the magenta-green CFA checker pattern. Figure 1.1.(a) is used in past papers and Figure 1.1.(b) shows the CFA of the test pixel array in this study. Since pursuing best color filter arrangement is not

Image Sensors and Imaging Systems 2015, edited by Ralf Widenhorn, Antoine Dupret,
Proc. of SPIE-IS&T Electronic Imaging, SPIE Vol. 9403, 940302 · © 2015 SPIE-IS&T
CCC code: 0277-786X/15/$18 • doi: 10.1117/12.2077122

the scope of this study, a simple color filter arrangement of a magenta-green alternate stripe is used. The VCT is covered with light shield metal, and it is located staggered array. In this study, we focused on a color signal variation in the 2LPDs that is enhanced by BSI process, especially backside thinning, and a crosstalk from adjacent pixels.

2. DEVICE STRUCTURE

Figure 2.1 shows the cross-section of a unit pixel in the test pixel array. The green pixel has the same structure with that for the conventional one. The magenta pixel consists of the 2LPD and the VCT. The 2LPD has the blue photo detector (B-PD) and red photo detector (R-PD). These are vertically integrated and electrically separated by charge separation layer. The 2LPD overlaid with the magenta color filter. The blue pixel is composed of the B-PD and the VCT. The B-PD is implemented on back-side surface to attain photo charges generated with shorter wavelength light. The VCT is made for the photo charges transfer from B-PD to charge storage region made near front side surface. The red pixel has the red photo diode (R-PD) that is made under the B-PD. Figure 2.2 shows test pixel layout and circuit diagram. This sensor is 12M 3-Tr Active Pixel Sensor, which has 2-shared pixels.

The B-PD is fabricated with high energy ion implantation of 31P ions from front side surface. The charge separation layer is made with high energy ion implantation of 11B ions from front side surface. The VCT and the R-PD are made with multiple step high energy 31P ion implantations. Other than these high energy ion implantation steps, ordinary bulk wafer BSI fabrication process is used to fabricate the test pixel array.

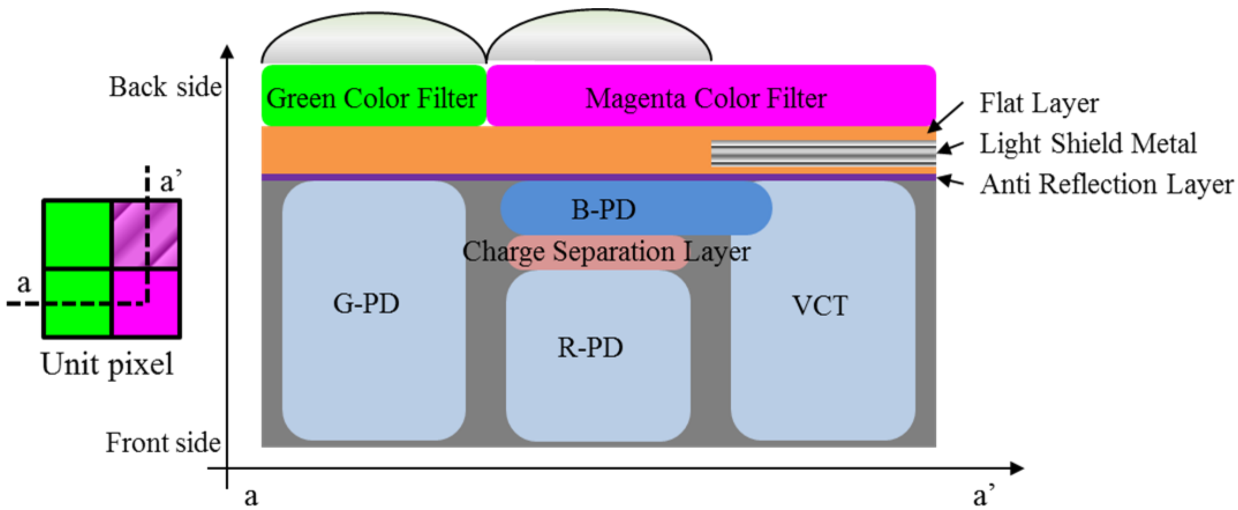

Figure 2.1 Device structure of a test pixel. The schematic is a sectional view taken along line a-a' of the Unit pixel.

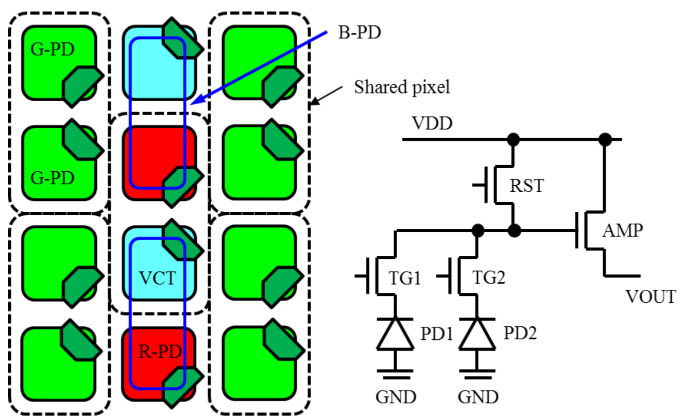

Figure 2.2 Test pixel layout and circuit diagram. 2-shared pixel is used in this sensor. In the test pixel layout, deep-green shows transfer gate, light-green shows G-PD, red shows R-PD, light-blue shows VCT, and blue rectangle shows B-PD region.

3. SPECTRAL RESPONSE AND SENSITIVITY

Figure 3.1.(a) shows spectral response of the test sensor and calculated data by light absorption theory. G is the response of the green pixel, which has 1LPD with green color filter. It is similar response to the green pixel in conventional BSI sensors. B is the response of the blue pixel, which has the B-PD of the 2LPD with magenta color filter and the VCT. The B-PD has the higher sensitivity as the shorter wavelength, because Silicon absorbs well as shorter wavelength. R is the response of the red pixel, which has the R-PD. The R-PD converts the photons that not absorbed the B-PD into the electrons, so the R-PD has the higher sensitivity at the longer wavelength. The 2LPD works as multi-color acquisition detector. Measured spectral response curves from 2LPD fitted well with those estimated based on light-absorption theory for Silicon detectors. The number of photons absorbed from depth t_1 to depth t_2 at wavelength λ, $N_{abs}(t_1, t_2, \lambda)$ is described by the formula:

$$N_{abs}(t_1, t_2, \lambda) = N_0(\lambda)(\exp(-\alpha(\lambda)t_1) - \exp(-\alpha(\lambda)t_2))$$

$N_0(\lambda)$ is the number of photons entering the silicon surface and $\alpha(\lambda)$ is the wavelength dependent absorption coefficient. In this study, $N_0(\lambda)$ is calculated by measured from 1LPD with magenta color filter. Figure 3.1.(b) is the Scanning Spreading Resistance Microscopy (SSRM) measurement result of the 2LPD in another sample, which made by the same process. The left photo is 2D resistivity map, in which the dark region shows the low resistivity. The right graph shows 1D resistivity plot of the gray straight line in 2D resistivity map. The photo detectors have high resistivity because it is depleted, so the saddle point of 1D resistivity plot shows the location of charge separation layer. In the case of this sample, the device thickness is 2.8um, and the charge separation layer is made at the depth of 1.90um seen from front side surface. The green dashed line in Figure 3.1.(a) is calculated by use of $t_1 = 0$, $t_2 = t_{si} = 2.8[um]$. The blue one is calculated by use of $t_1 = 0$, $t_2 = t_{BPD} = 0.9[um]$. The red one is calculated by use of $t_1 = t_{BPD} = 0.9[um]$, $t_2 = t_{Si} = 2.8[um]$. Controlling both the depth of the charge separation layer and the thickness of the BSI wafer, spectral response of the 2LPD is optimized as both low crosstalk and high QE are attained.

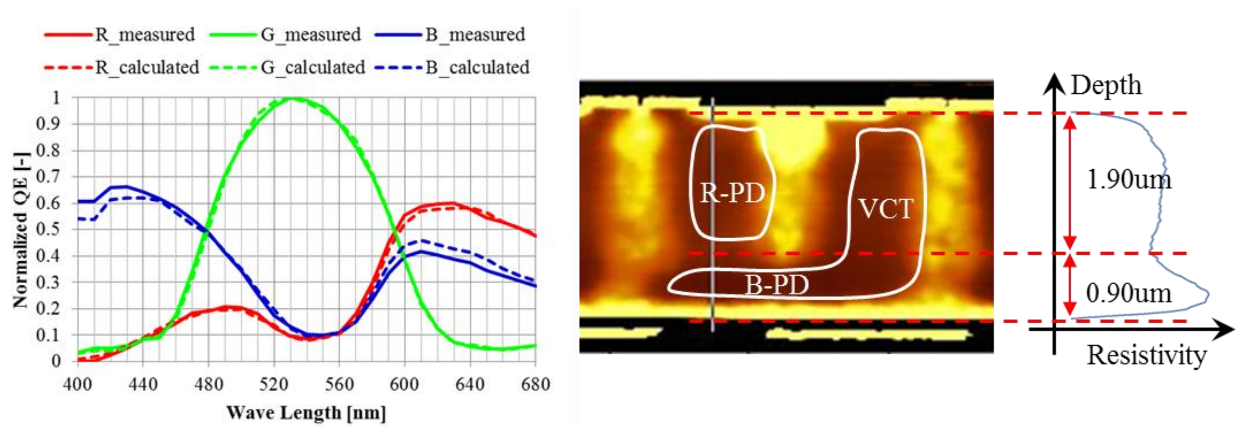

(a) (b)

Figure 3.1 (a)Spectral response of the 2LPD. The Straight line shows the measurement data of the test sample. The dashed line shows the calculated data by light-absorption theory, which is used $t_{BPD} = 0.9[um]$ and $t_{Si} = 2.8[um]$. The value of vertical axis is normalized at peak value of green pixel. (b) SSRM measurement result of the 2LPD. The left photo is 2D resistivity map; the right graph shows 1D resistivity plot of the gray straight line in 2D resistivity map.

The 2LPD architecture has higher sensitivity than the Bayer one. The stacked bar chart in Figure 3.2 shows the normalized sensitivity of blue and red pixels in three different samples. “1LPD” is a Bayer type sample. (a) shows the sensitivity of the 1LPD with red CF, (b) shows that of the 1LPD with blue CF. “2LPD (1:1)” is the test sensor has 2LPD with magenta CF, which has the same width of VCT as R-PD. (c) shows the sensitivity of the red pixel, (d) shows the sensitivity of the blue pixel. Photo electrons generated in Magenta pixel are shared by the 2LPD and blue signal is successfully transferred out via VCT. Despite the half of the aperture ratio, “2LPD (1:1)” has a similar amount of sensitivity as “1LPD”, because magenta CF transmits wide-band wavelength. This result shows that the 2LPD, which has higher aperture ratio than the half one, has the higher sensitivity than the 1LPD. “2LPD (1.5:0.5)” is the test sensor has 2LPD, which has the half width of VCT as R-PD. The sensitivity of this sensor is about one and half times that of "1LPD". Implementation of the narrow width VCT is key technology on high performance 2LPD.

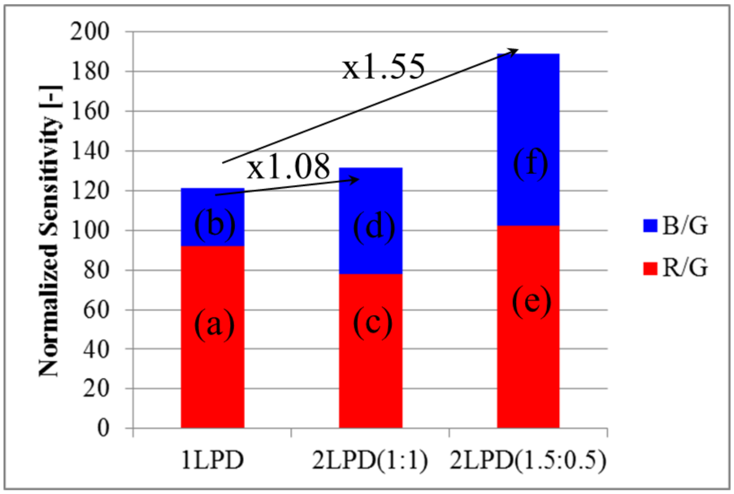

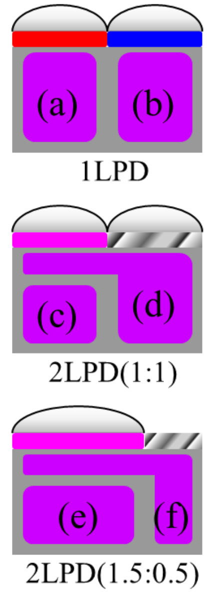

Figure 3.2 The normalized sensitivity of Blue and Red pixels with IR 650 filter, 2850K illuminant. The sensitivity is normalized at the one of green pixel in the same sample, which has 1LPD. The right pictures show the cross section schematics of three different structures. "1LPD" and "2LPD(1:1)" has circular micro-lenses, "2LPD(1.5:0.5)" has oval micro-lense.

4. BACKSIDE THINNING

Spectral response of the 2LPD is controlled by both the depth of the charge separation layer and the thickness of the BSI wafer. We fabricated different thickness of 2LPDs. Figure 4.1.(a) compares normalized QE curves for Si thickness of 2.5um and of 2.8um. The straight lines shows the response of $t_{si} = 2.8[um]$, the dashed line shows the response of $t_{si} = 2.5[um]$. QE curves varied with Si thickness because the depth of charge separation layer seen from backside surface changes as Si thickness changes. The thinner Si is, the closer to backside surface the charge separation layer is located. The B-PD becomes thinner, the sensitivity of the B-PD decreases. The R-PD is closer to backside surface, the sensitivity of R-PD increases. Color signal dependency on Si thickness is shown in Figure 4.1.(b). Color signals are normalized at respective values at 2.8um Si thickness. Compared 2.5um to 2.8um, normalized sensitivity of Green in 1LPD decreased 97%, whereas that of Blue in 2LPD decreased 80% and that of Red in 2LPD increased 125%. It's shown that blue and red pixels of the 2LPD are sensitive to Si thickness variance. In a practical situation, the major cause of Si thickness variation is backside thinning process. This result shows that a variation of backside thinning in BSI process is caused a great color signal variation.

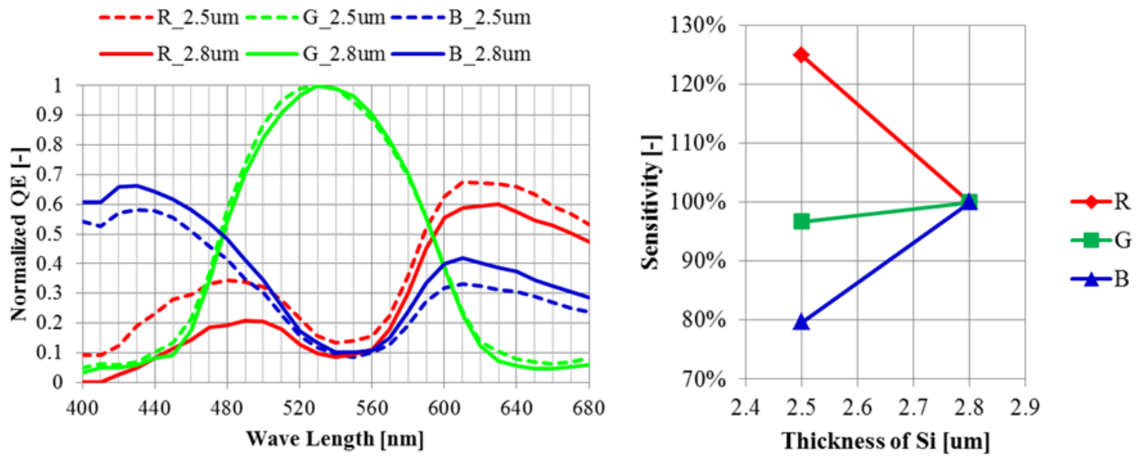

(a) (b)

Figure 4.1 The left graph shows Spectral responses of the 2LPDs, which has different thickness. The value of vertical axis is normalized at peak value of green pixel. The right graph shows that the sensitivity dependency on Si thickness with IR 650 filter, 2850K illuminant, integration value of the sensitivity in a wavelength region of 400nm to 680. Color signals are normalized at respective values at 2.8um

5. CROSSTALK

The light shielding metal coverage should be smaller due to the large aperture of the 2LPD, when the 2LPD architecture is implemented in a smaller pixel than 2.2um. To provide guidelines for the consideration of the design rule of the light shielding metal coverage, we made two types of crosstalk-monitor patterns. Figure 5.1(a) shows the wide width VCT pattern "2LPD(1:1)" that has the same width of VCT as R-PD, Figure 5.1(b) shows the narrow width VCT pattern "2LPD(1.5:0.5)" that has the half width of VCT than the former. There are several types of the light shielding metal coverage in each pattern. By use of these patterns, the cross-talk to the VCT from adjacent pixels is evaluated.

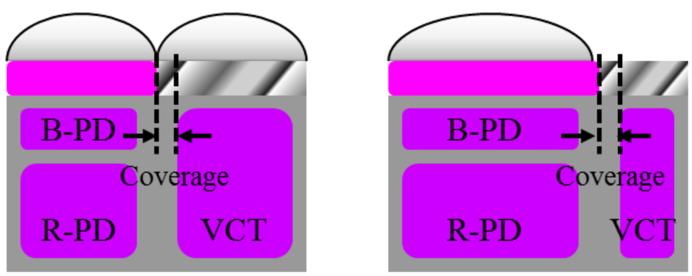

(a) 2LPD(1:1) (b) 2LPD(1.5:0.5)

Figure 5.1 (a) "2LPD(1:1)" shows the same width of VCT as R-PD, this one has circular micro-lenses. (b) "2LPD(1.5:0.5)" shows the half width of VCT as (a), this one has oval micro-lenses. The B-PD in each pattern is connected with the G-PD.

Figure 5.2 shows crosstalk dependency on light shielding metal coverage. When the light shielding metal coverage is 0, the edge of the metal is at the boundary between R-PD and VCT. When the light shielding metal coverage has plus value, then metal edge is on R-PD. The crosstalk from adjacent pixels to VCT decreases with metal shield edge. Light shielding metal coverage should be smaller otherwise optical aperture of Magenta pixel decreases and hence QE for magenta pixel gets lower. The narrow width VCT shows high amount of cross-talk. One of the possible reasons why cross-talk increased is oval micro-lenses. It is expected that the long direction of the oval micro-lenses is poor condensing. The narrow width VCT needs larger amount of coverage than the wide width VCT. Therefore, to achieve low crosstalk structure for the VCT is one of the key issues for BSI 2LPD architecture.

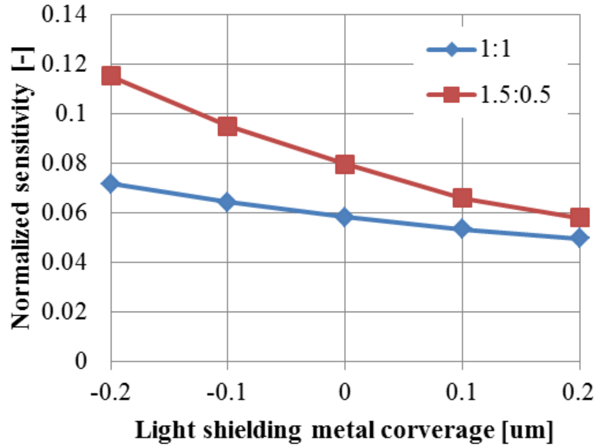

Figure 5.2 Crosstalk dependence on light-shielding metal coverage with IR 650 filter, 2850K illuminant. The blue line shows the same width of VCT as R-PD, the red one shows the half width of VCT than the former. The Sensitivity is normalized at the one of green pixel in the same sample, which has 1LPD.

6. CONCLUSIONS

This paper reports on a study of the 2LPD structure implemented in BSI architecture to see a feasibility of a small pixel 2LPD BSI as a possible solution for better low light SNR. The 2LPDs test pixel array has been successfully demonstrated for 2.2um BSI CMOS image sensor. The measured spectral response curves with blue/red two layer stacked photo diode is close to those estimated based on simple light-absorption theory for Silicon detectors. It's found that crosstalk to VCT path is an important key factor to realize BSI 2LPD pixel. To achieve very small pixel such as sub-micron size pixels, alternative isolation technology such as Deep Trench Isolation (DTI) might be necessary to reduce a crosstalk to the VCT [7]. Also it's found that considerably large color signal variation is caused by Si photo detector thickness variance. Minimizing Si thickness variance due to backside thinning process is one of the key issues to realize BSI 2LPD pixel.

REFERENCES

[1] Bayer, B. E. "Color Imaging Array," U.S.Patent, 3,971,065, (1976).

[2] Merrill, R., "Color Separation in an Active Pixel Cell Imaging Array Using a Triple well Structure," U.S.Patent, 5,965,875, (1999).

[3] Lyon, R., Hubel, P., "Eyeing the Camera: Into the Next Century," IS&T/TSID 10th Color Imaging Conference Proceedings, 349-355, (2002).

[4] Findlater, K. M., Renshaw, D., Hurwitz, J.E.D., Henderson, R.K., Purcell, M.D., Smith, S.G. and Bailey, T.E.R., "A CMOS image sensor with a double-junction active pixel," IEEE Transactions on Electron Devices, 50(1), 32-42 (2003).

[5] Tweet, D. J., Lee, J. -., Speigle, J. M. and Tamburrino, D., "2PFCTM Image Sensors: Better Image Quality at Lower Cost," Proc. SPIE 7250, 725007 (2009).

[6] Fossum, E.R., "Investigation of Two-Layer Photodetectors for YNSR10 Improvement in Submicron Pixels," Proceedings of International Image Sensor Workshop, (2011).

[7] Y.Kitamura, et al., "Suppression of crosstalk by using backside deep trench isolation for 1.12um backside illuminated CMOS image sensor," the Technical Digest - International Electron Devices Meeting, IEDM, 24.2.1-24.2.4., (2012)